Search for spin-polarized photoemission from GaAs using light with orbital angular momentum

N. B. Clayburn,[1] J. L. McCarter,[2] J. M. Dreiling,[1] M. Poelker,[3] D. M. Ryan,[1] and T. J. Gay[1]
[1]*Jorgensen Hall, University of Nebraska, Lincoln, Nebraska 68588-0299, USA*
[2]*Department of Physics, University of Virginia, Charlottesville, Virginia 22904-4714, USA*
[3]*Thomas Jefferson National Accelerator Facility, 12000 Jefferson Avenue, Newport News, Virginia 23606, USA*
(Received 14 August 2012; revised manuscript received 29 November 2012; published 22 January 2013)

Laser light with photon energy near the band gap of GaAs and in Laguerre-Gaussian modes with different amounts of orbital angular momentum was used to produce photoemission from unstrained GaAs. The degree of electron spin polarization was measured using a micro-Mott polarimeter and found to be consistent with zero with an upper limit of ∼3% for light with up to $\pm 5\hbar$ of orbital angular momentum. In contrast, the degree of spin polarization of 32.3 ± 1.4% using circularly polarized laser light at the as the same wavelength, which is typical for bulk GaAs photocathodes.

DOI: 10.1103/PhysRevB.87.035204 PACS number(s): 42.50.Tx, 34.80.Nz, 79.60.Bm, 07.77.Ka

I. INTRODUCTION

A light beam with azimuthal phase dependence—often referred to as "twisted light"—can carry orbital angular momentum (OAM) about its axis of propagation. This phase dependence corresponds to a helical path for the beam's Poynting vector.[1] Light with OAM is different from conventional circularly polarized light that possesses only one unit ($\pm\hbar$) of spin angular momentum (SAM) per photon in that it can possess arbitrarily large values of OAM, $\pm m\hbar$, where m is a positive integer.

GaAs has long been used to generate spin-polarized electron beams via photoemission using light with SAM.[2] These electron beams are created using atomically clean GaAs in an ultrahigh vacuum environment. Photoemission is obtained when chemicals (e.g., Cs and NF_3) are applied to the surface to produce a negative electron affinity (NEA) condition. When circularly polarized light with near-band-gap energy illuminates the GaAs, spin-polarized electrons are emitted.[3] The degree of polarization, relative to an arbitrary axis of quantization, is defined to be

$$P = \frac{N\uparrow - N\downarrow}{N\uparrow + N\downarrow}, \tag{1}$$

with $N\uparrow$ and $N\downarrow$ being the number of electrons with spin up and spin down, respectively.

For unstrained GaAs, the theoretical maximum polarization is 50%, but in practice polarization is typically 25–35% due to various depolarization mechanisms.[3] Significantly higher polarization can be obtained from thin, strained GaAs,[4–6] in which the strain serves to eliminate the light-hole/heavy-hole degeneracy at the Γ point in the ground state, thereby providing a means to selectively populate the conduction band with a higher percentage of electrons with the desired spin. Polarization >80% is now relatively common with such materials, but the photoemission yield per incident photon—or quantum efficiency (QE)—is rather small (<1%). However, advances continue to be made; there are recent reports of QEs in excess of 1% together with polarization in the 85–90% range using GaAs-based superlattice photocathodes.[7] Many physics programs would benefit greatly from photocathodes that provide high polarization with a better QE.

In this paper, we explore the idea of creating spin-polarized electron beams by imparting angular momentum to electrons in the conduction band of regular, bulk GaAs using light with OAM. Such an idea is appealing; given the large amount of OAM that vortex beams can carry, one might expect that at least part of it could be transferred through spin-orbit coupling to the photoelectrons emitted from the surface. This paper presents the results of experiments to test this idea. Our polarization measurements were consistent with zero, suggesting that light with OAM does not couple effectively to the internal motion of electrons in a semiconductor, at least when the focused transverse laser spot size is ∼200 μm or larger.

II. THEORETICAL CONSIDERATIONS

To date, only quasimacroscopic systems, such as dust particles, have been shown to interact directly with OAM.[8] Searches for transfer of OAM to atomic and molecular systems have as yet yielded no measurable results.[9] Qualitatively, one might expect efficient OAM coupling to a target only when the target's spatial scale is comparable to that of spatial variations in the intensity pattern of the laser beam associated with the OAM, i.e., the target must be big enough to "sense" that it is in a beam with OAM. In our case, we used beams with Laguerre-Gaussian (LG) modes whose field amplitude is given by the complex scalar function[1]

$$\mathrm{A}_{pm}(r,\varphi,z) = \mathrm{C}\left[\frac{r\sqrt{2}}{\alpha}\right]^m L_p^m\left[\frac{2r^2}{\alpha^2}\right] \times e^{-\frac{r^2}{\alpha^2}} e^{\frac{ikr^2}{\beta}} e^{-im\varphi} e^{i(2p+m+1)\gamma}, \tag{2}$$

where r, φ, and z are the standard cylindrical coordinates for the beam, C, α, β, and γ are z-dependent parameters, L_p^m is an associated Laguerre polynomial, m is the azimuthal index corresponding to $m\hbar$ of OAM per photon, and p is the beam's number of radial nodes. For LG laser modes, the radius of maximum intensity for diffraction-limited focusing is approximately $w_0\sqrt{m/2}$, where w_0 is the Gaussian beam waist.[10] However, when considering the interaction between fields possessing OAM and atomic systems, the relevant spatial scale is of the order of $\lambda/2\pi$, where λ is the light's wavelength.[11–13]

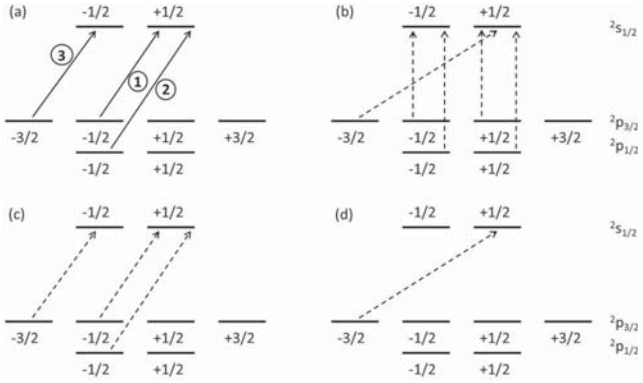

FIG. 1. Energy level diagram for unstained bulk GaAs. The values of m_j are indicated below or above the respective states. In (a) the solid arrows indicate transitions caused by absorption of circularly polarized light with SAM of $+1\hbar$; the circled numbers associated with these transitions indicate their relative transition strengths. These lead to a maximum ^2s upper-state polarization of 50% if absorption occurs exclusively from the $^2p_{3/2}$ levels. In (b)–(d) possible transitions for linearly polarized light with OAM $= +1, +2$, or $+3$, respectively, are shown (see text). The dashed arrows correspond to vector addition of SAM of both $+1\hbar$ or $-1\hbar$ and OAM, as linearly polarized light is composed of photons of both spin states.

Now consider the simplified energy-level diagram for GaAs shown in Fig. 1.[2] The ground state valence-band states possess p-symmetry at the Γ point, with the $^2p_{1/2}$ and $^2p_{3/2}$ states being split by spin-orbit interaction. The standard technique for the production of spin-polarized electrons by photoemission from GaAs relies on the absorption of circularly polarized light with SAM of, e.g., $+1\hbar$, where electrons make transitions to the conduction band states of ^2s symmetry proportional to the respective transition strengths indicated by the labels 1, 2, and 3 in Fig. 1(a). We are interested in an experimental answer to the question: can a beam of linearly polarized light, which has average SAM $= 0$, but with OAM $= +1\hbar$, pump these electric dipole transitions at the Γ point as well? Because photons are massless vector bosons, linearly polarized light must be ultimately absorbed with a transfer of either $+1\hbar$ or $-1\hbar$ of SAM. Thus, the net transfer of angular momentum to the target for absorption of a given photon must in this case be either 0 or $+2\hbar$ for angular momentum to be conserved [Fig. 1(b)]:

$$\text{OAM} + \text{SAM} = \Delta m_j. \tag{3}$$

By requiring conservation of angular momentum, one could envision, e.g., absorption of linearly polarized light with (average) SAM $= 0$ but with OAM $= +3\hbar$ [Fig. 1(d)] leading to a net absorption of $+2\hbar$ exclusively from the $m_j = -3/2$ state. Would this yield a higher polarization, given that only the upper $^2s_{1/2}$, $m_j = +1/2$ state would be populated? In principle, by absorbing angular momentum into the higher angular momentum components of the Bloch wave functions away from the Γ point, even higher OAM might be coupled into the system. Could this produce even higher electron polarization? Or, perhaps the extra angular momentum would be absorbed directly in other, collective modes of excitation, such as excitons or phonons not explicitly designated in Fig. 1 so that

$$\text{OAM} + \text{SAM} = \Delta m_j + \Delta m_{J(\text{other})}, \tag{4}$$

where J(other) labels the total (spin plus orbital) angular momentum of the lattice as a whole other than that due to conduction electron waves in the immediate vicinity of the Γ point.

If coupling between electron spin and OAM light does occur, the natural question of transition probabilities arises. Although the theoretical transition strengths for the polarized light at the Γ point are straightforward to calculate,[2] the associated probabilities for transitions involving OAM [Figs. 1(b)–1(d)] have not been published to our knowledge.

We note that we have neglected the effects of parity conservation, i.e., Laporte's rule, which would further restrict the allowed transitions. This is valid as Laporte's rule applies strictly only to centrosymmetric systems and not to semiconductors such as GaAs that do not possess an inversion center, except precisely at the Γ point.

To our knowledge, no analysis has considered the state-to-state optical pumping of semiconductors with light having OAM, although a number of authors have considered absorption of OAM light by atoms and molecules.[11–13] When the center-of-mass motion of the absorbing system is taken into account in these latter cases, light of arbitrarily high OAM can be absorbed. For electric dipole and electric quadrupole transitions, the transition probability P has been shown to be

$$P\alpha\left(\frac{2\pi\,\Delta x}{\lambda}\right)^{2m-2}, \tag{5}$$

where Δx is roughly the size of the atomic or molecular target's de Broglie wave packet.[11,12] In general, for atomic or molecular targets, $(2\pi\,\Delta x/\lambda)$ is approximately 10^{-3}. In the case of a semiconductor, Δx corresponds more naturally to the size of the extended Bloch electron wave functions. Due to k mixing caused by impurities or scattering from polarons, Δx is typically of the order of 1–10 nm,[14] which increases $(2\pi\,\Delta x/\lambda)$ to perhaps as much as 10^{-2}. However, if $m = 1$, the quantity $(2\pi\,\Delta x/\lambda)^{2m-2}$ is of the order unity and independent of Δx. This means that for transitions involving an OAM of $1\hbar$, transition rates could reasonably be expected to not be vanishingly small. This picture is muddled somewhat by a disagreement (albeit for molecular targets) between Refs. 11 and 13 about whether electric dipole transitions with one unit of OAM can be expected to be significant.

An alternate approach has considered electrons that are promoted to the conduction band from the heavy-hole valence band by absorption of OAM light to be free carriers.[15] The OAM of the incident beam produces electric currents in the bulk that, in turn, set up magnetic fields. Only the case with $m = 1$ appears to set up currents that give a net spatial circulation around the beam axis. For a pulsed laser with wavelength of 1000 nm and a pulse energy of 3 μJ over 10 fs, with a spot size of $\sim(0.5\ \mu\text{m})^2$, the authors of Ref. 15 calculate at the photon absorption depth a field of $\sim$10 G due to these free currents. Even with this very tight focus, such a field seems too small to affect (or, more importantly, to produce) the spin polarization of electrons emitted from the surface in the subpicosecond transport times required.

Given the paucity and tenuous connection of the calculations available in the literature with the situation we consider, we decided to explore OAM-carrier-electron coupling experimentally.

III. EXPERIMENT

In our experiment, two linearly polarized laser beams of comparable intensity were directed at diffraction gratings with screw dislocations to produce two linearly polarized laser beams with LG transverse spatial modes.[1,16–19] The amount of the OAM was determined by the choice of grating, and the two beams had opposite senses of rotation. The light was then directed to a GaAs photocathode to produce electron beams that were delivered to a compact retarding-field micro-Mott polarimeter.[20]

A. Electron source and polarimeter

The experimental apparatus consisted of three main sections (Fig. 2): a source chamber for installing and activating the photocathode, a transport section for steering the electron beam to the polarimeter, and the Mott polarimeter. The photocathode was thick, unstrained GaAs with a (100) surface crystal orientation, a Zn dopant concentration of 5×10^{18} cm^{-3}, and an etch pit density $\sim$5000 cm^{-2}. Surface preparation of the photocathode consisted of heating to $\sim$550 °C for 1 hr, cooling to room temperature, and then coating with approximately one monolayer of Cs and NF_3 to achieve a NEA surface condition. The maximum QE of the photocathode was $\sim$8% at 789 nm. Following activation, it was lowered into the transport section of the apparatus and biased at -268 V. Laser light illuminated the photocathode from below, and the photoemitted electron beam was deflected toward the micro-Mott polarimeter using a simple electrostatic deflector.[21] As a result of this $\sim$90° deflection, the electron spin was changed from a longitudinal to a transverse orientation, which is a necessary condition for Mott-scattering polarimetery. Additional electrostatic deflectors and lenses were used to facilitate the delivery of the electron beam to a thick gold target inside the polarimeter.

In general, both the efficiency of transport of the electron beam from the photocathode to the Mott polarimeter and the QE of the photocathode are functions of the position on the photocathode hit by the laser beam. The latter can be determined by the measurement of total photoemission current as a function of this position, and the ratio of the current detected at the Mott polarimeter to that emitted from the photocathode yields the transmission efficiency. In our experiment, we generated electron beams from a region of the GaAs crystal that was characterized by both spatially constant QE ($\sim$8%) and transmission ($\sim$23%). This region was approximately circular with a $\sim$2-mm diameter, i.e., significantly bigger than any focal spot of the laser beam that we used in our experiments.

For electron polarization measurements using conventional circularly polarized light, an asymmetry, A, for electrons scattered from the Mott target was constructed:

$$A \equiv \frac{N^+ - N^-}{N^+ + N^-}, \tag{6}$$

where $N^+ = \sqrt{L_+ R_-}$ and $N^- = \sqrt{L_- R_+}$, with L and R representing the number of electrons detected by the left and right channel electron multipliers (CEMs), while "+" and "−" refer to the helicity of the circularly polarized light. This way of constructing A serves to significantly reduce instrumental asymmetries due to, e.g., different CEM detection efficiencies or helicity-related beam intensities.[22] The electron polarization P_e is given by $P_e = A/S_{\text{eff}}$, where S_{eff}, the effective Sherman function, is the polarimeter's analyzing power. For polarization measurements using photoemission generated with OAM, the same formulism was used with the "+" and "−" spin states now referring to illumination of the photocathode with two different laser beams having LG spatial modes of opposite rotational sense.

B. Laser system

A simple laser system was used to generate polarized photoemission using circularly polarized light (Fig. 3). Linearly polarized light from a 789-nm, 30-mW diode laser was focused, passed through a pinhole spatial filter, collimated, and then directed to the photocathode using steering mirrors. Laser power at the photocathode was adjusted via an optical attenuator consisting of a linear polarizer, rotatable birefringent $\lambda/2$ plate, and another fixed linear polarizer. A laser power of <1 μW was chosen to obtain the desired CEM count rate. Downstream of the attenuator was a fixed $\lambda/4$ plate oriented to produce $\sim$100% circularly polarized light. A computer-controlled $\lambda/2$ plate could be inserted immediately upstream of the fixed $\lambda/4$ plate to flip the

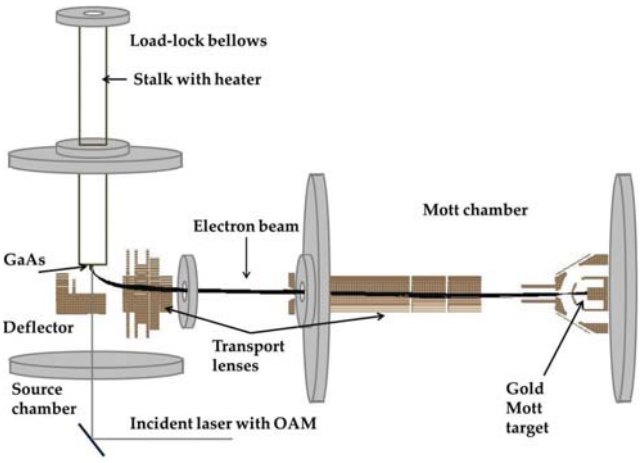

FIG. 2. (Color online) Schematic of the experimental apparatus used to measure the polarization of electrons emitted by OAM light excitation of NEA GaAs.

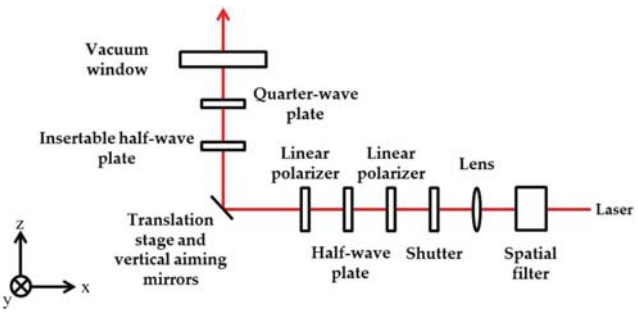

FIG. 3. (Color online) Schematic of the optical system used to generate polarized photoemission using circularly polarized light.

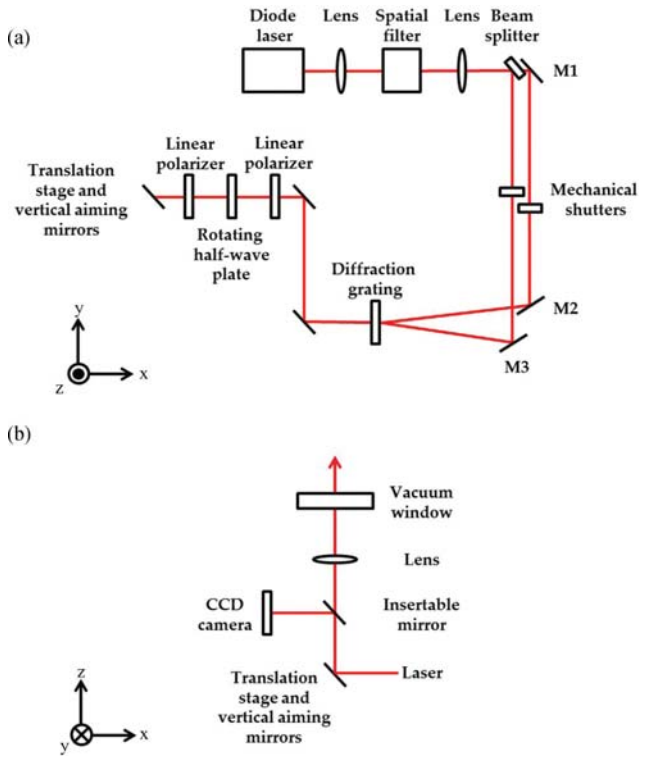

FIG. 4. (Color online) Schematic of the optical system used to generate polarized photoemission using OAM light; (a) shows the components of the horizontal section of the optical system in the xy plane, while (b) shows the components of the vertical section in the xz plane. The diffraction grating can be removed completely and replaced with gratings of different topological charge (see text). Steering mirrors M1, M2, and M3 and the beam splitter were adjusted to align companion OAM beams at the same location; this alignment was verified by using the insertable mirror which delivered the beams to the CCD camera (see text).

helicity of the circularly polarized light at the photocathode. The position of the light on the photocathode could be adjusted by moving the last two steering mirrors, which were attached to computer-controlled stepper-motor translation stages. Finally, a lens was used to focus the light on the photocathode.

The $\lambda/4$ plate and insertable $\lambda/2$ plate were not used to generate light with OAM. Instead, the two $\pm$OAM states were produced by creating two independent linearly polarized laser beams using a 50/50 beam splitter [Fig. 4(a)]. These beams were delivered one at a time at opposite incident angles to a diffraction grating manufactured with a fringe defect (Fig. 5).[16–19] The diffraction gratings were fabricated by transferring a computer-generated interference pattern to a transparent photographic film using a film camera. The interference patterns are holograms created using a plane wave and an optical vortex with OAM of $\pm m\hbar$, where m is the topological charge of the vortex and indicates the number of phase windings along the axis of propagation. The sign multiplying m denotes the sense of rotation: "$+$" indicates clockwise rotation while looking into the beam, and "$-$" indicates counterclockwise rotation.

Full illumination of an m-fringe defect of the grating produces multiple downstream beams: a central undeflected

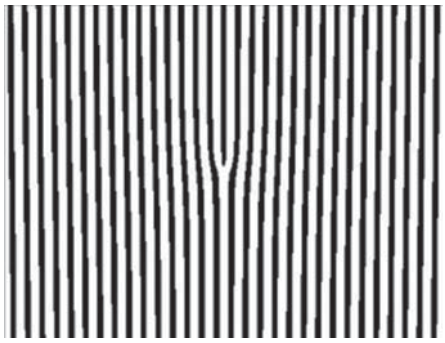

FIG. 5. Computer-generated $m = 1$ interference pattern comprising alternating dark and light fringes. The unperturbed fringes define the vertical axis of the grating. The order 1 fringe defect is apparent in the center of the figure.

fundamental Gaussian beam (diffraction order $n = 0$) and adjacent beams corresponding to higher-order diffraction modes separated by small angles and carrying OAM of $n \cdot m\hbar$. These output beams are superpositions of LG modes with the same azimuthal index m, but different numbers (p) of radial nodes, with $p = 0$ being the predominant value. The angle between diffraction orders depends on the number of lines per centimeter of the grating in regions well away from the fringe defect, similar to a regular diffraction grating. Only the beams of diffraction order $n = \pm 1$ were used in these experiments; the central undeflected beam and higher-order modes were blocked. An electron polarization measurement for light with $m\hbar$ of OAM consisted of illuminating the appropriate grating with two different light beams incident on the grating at angles corresponding to diffraction orders of ± 1 [Fig. 4(a)]. The beams were directed at the photocathode, and the polarization of the emitted electron beam was then determined using Eq. (6). Companion polarization measurements were made with each diffraction grating rotated 180° about its vertical axis to flip the OAM spin direction.

As mentioned above, light beams with OAM have a dark center surrounded by a bright concentric ring of light when projected on a screen, creating an annular pattern. To ensure that the two beams with positive and negative OAM strike the photocathode at the same location, the beams were alternatively delivered to a charge-coupled device (CCD) camera [Fig. 4(b)] by inserting a deflecting mirror just before the vacuum window. The camera was positioned at the same distance from the grating (as measured along the appropriate optical path) as the photocathode. The steering mirrors M1, M2, and M3, as well as the beam splitter, were adjusted to align the two OAM beams to the same location on the camera, and the position of the grating was adjusted to obtain the most uniform LG spatial modes. Examples of OAM states with $m = 1$, 2, 3, and 5 are shown in Fig. 6. Also pictured in Fig. 6 are interference patterns generated by superimposing positive and negative OAM beams of charge m. A helical wave front that interferes with its mirror image results in $2m$ dark fringes. These interferograms provide an easy means to confirm the charge, m, of any LG mode.

The CCD camera also provided a measure of the size of the laser beam at the photocathode for each OAM state, which varied significantly with m (Table I). A lens was empirically

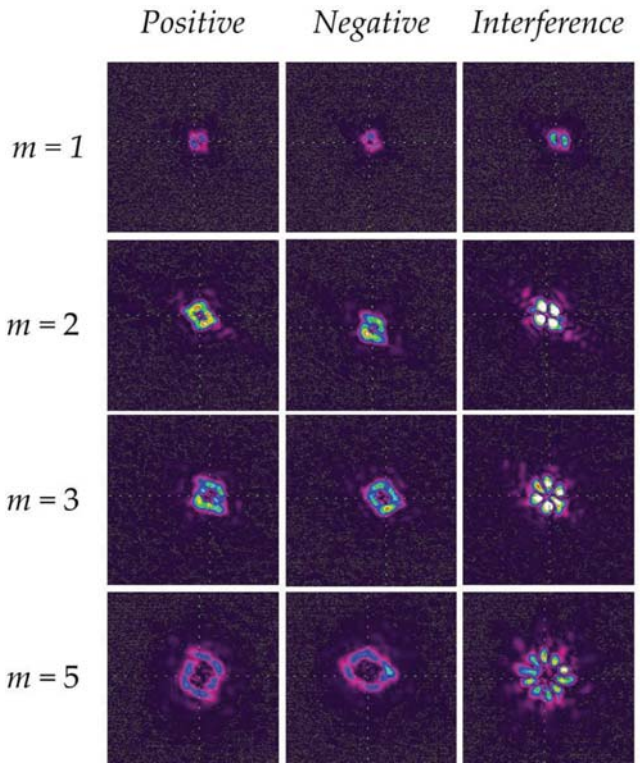

FIG. 6. (Color online) Intensity patterns of various OAM beams taken by the CCD camera (see text). The integer number m is the topological charge of the vortex. In the rightmost column are the interference patterns obtained by superimposing the positive and negative OAM beams which reveals their "vortex" nature. See also Table I.

selected to achieve the tightest spot at the GaAs photocathode for the $m = 2$ grating, and the same lens was then used for all other measurements. The spot size measurement by the CCD for the $m = 2$ grating was confirmed using a moveable knife edge. Based on Eq. (5) and the fact that w_0 is proportional to λ, the tightest focusing was assumed to provide the greatest opportunity to observe polarized photoemission. It also served to minimize any systematic error associated with variation in the QE or efficiency of transmission to the Mott polarimeter due to the location of emission from the photocathode. We note that, as discussed in Sec. II, the focal spot size (Table I) varies roughly as $\sqrt{m}$, while the spatial scale of beam intensity variation (Fig. 6) is approximately constant and independent of m. The focused spots sizes for the OAM laser beams ranged from ~250- to 750-μm full width at half-maximum (FWHM). For a pure Gaussian beam, the diffraction-limited spot size would be on the order of ~100 μm, when accounting for the collimated laser beam size and the focal length of the lens that was used.

TABLE I. FWHM measurements of the focused OAM beams from CCD camera images taken at the same distance from the grating (as measured along the appropriate optical path) as the photocathode.

Units of OAM	Width (μm)	Height (μm)
+1	273	215
−1	313	315
+2	377	436
−2	378	382
+3	488	443
−3	536	495
+5	719	745
−5	842	680

IV. RESULTS

A. Beam absorption

Given the discussion of Sec. II and from a simple analysis of Fig. 1, one might be tempted to conclude that absorption (and hence QE) of linearly polarized light with average SAM $= 0$ and $m > 3$ would be severely suppressed. This is apparently not the case. While we made no quantitative measurements of photocathode QE vs m, we did not notice large differences in the photocurrent that could be extracted as the beam's OAM was varied. Since, as we shall see, the photoemitted electrons take up essentially none of the OAM of the incident laser beam, the question naturally arises as to the ultimate dynamical mechanism whereby angular momentum of the system is conserved. We speculate that the light's OAM couples to the free conduction-band electron carriers,[15] which, in turn, couple to phonon motion.

B. Beam polarization using conventional circularly polarized light

The functionality of the apparatus, and in particular the retarding-field Mott polarimeter, was verified using circularly polarized laser light (Fig. 3). The photocurrent at 10^{-9} A levels was delivered to the Mott target, which was biased at $+20$ kV. As mentioned above, the electron beam polarization is related to the measured count asymmetry by $P_e = A/S_{\text{eff}}$, where S_{eff} was determined previously to be 0.201 ± 0.005.[20] The value of S_{eff} is a function of ΔE, which is the largest amount of inelastic energy loss an incident electron can have suffered in the target and still be detected by the CEMs.[20,22] This maximum energy loss ΔE can be varied by adjusting the bias voltage applied to grids at the entrance of the CEMs. The value of $S_{\text{eff}}(\Delta E)$ increases with decreasing ΔE because inelastic scattering events, which depolarize the detected electrons, are increasingly discriminated against. In practice, the count rates for purely elastic scattering are very low, so the S_{eff} quoted above was determined by linearly extrapolating values of $S_{\text{eff}}(\Delta E)$ to $\Delta E = 0$. We note, however, that S_{eff} $(\Delta E = 0)$ is generally less than the elastic scattering single-atom limit.[22]

Repeated asymmetry measurements were made as ΔE was varied. At the maximum grid voltage of -268 V (which corresponds to the bias voltage of the photocathode), $\Delta E = 0$ and only elastically scattered electrons reach the detectors. Similar to the procedure discussed above, the quoted asymmetry is determined by linearly extrapolating values of A to $\Delta E = 0$. Detector background subtractions for the residual rate with no laser light were made along with subtraction of the residual rate when the retarding field exceeded that required to exclude elastically scattered electrons. Figure 7 shows asymmetry data and a ΔE extrapolation linear fit for 20-kV target bias for both circularly polarized light and linearly polarized light with OAM.

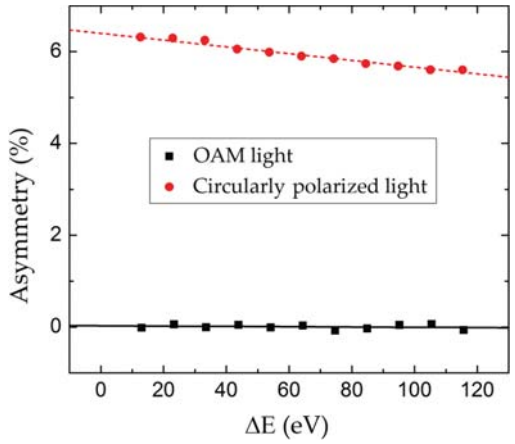

FIG. 7. (Color online) Asymmetry as a function of ΔE for OAM light and circularly polarized light. Solid and dashed lines indicate the weighted linear fit for extrapolation to $\Delta E = 0$ eV for OAM and circularly polarized light, respectively. Error bars are smaller than the data points.

C. Beam polarization using OAM light

Four different diffraction gratings were used to create light with ± 1, ± 2, ± 3, or ± 5 units of OAM. Repeated polarization measurements, shown in Fig. 8, indicate that the polarization for all topological charges is less than $\sim 3\%$ and is consistent with zero. The error bars reflect an absolute uncertainty of $\pm 0.05\%$ in the polarization measurements as well as an absolute systematic uncertainty of $\pm 1.77\%$ (added linearly). The latter systematic uncertainty was determined as discussed below and is completely dominated by effects associated with changes in the spatial profile of the OAM light on the photocathode as the sign of the topological charge is flipped. The polarization uncertainty is a linear combination of systematic error associated with S_{eff} and the random statistical uncertainty in the measurement of A.

An analysis of the effect of incident light linear polarization angle on any possible electron polarization was conducted for the $\pm 2\hbar$ OAM beam by rotating the linear polarizer closest to the vacuum window [Fig. 4(a)]. Within statistical uncertainties, the electron polarization variation due to this was found to be negligible (Fig. 9). In another systematic study, no significant polarization variation was obtained by varying the size of the laser focus at the photocathode for a topological of charge of $m = 2$ (Fig. 10), thus establishing that small variations in spot size near the diffraction-limited regime do not affect the measured polarization.

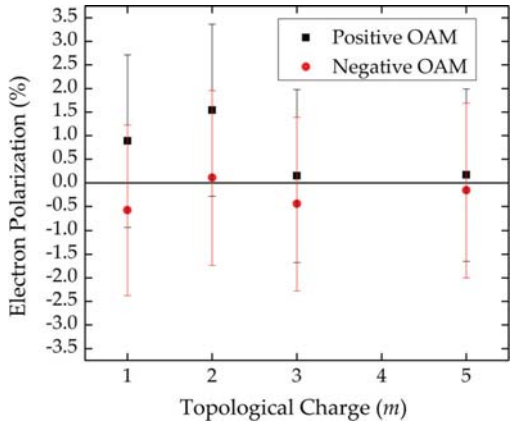

FIG. 8. (Color online) Electron polarization measurements for beams with various amounts of OAM. Error bars are discussed in the text.

Returning to Fig. 8, we note that if only the polarization uncertainty of 0.05% is considered, there is a residual polarization difference between the positive and negative OAM results, at least for $m = 1$ and $m = 2$. However, systematic uncertainties due to laser misalignment between the opposite charge states completely obscure any possible real electron polarization. These laser misalignments result in small associated differences in average QE as well as electron beam transport efficiency to the Mott CEMs. The images in Fig. 6 make it clear that the OAM beams possess noticeable differences in their intensity profiles and do not have perfect LG modes. For instance, the $m = 2$ beams have intensity minima and maxima at diametrically opposite locations. As m increases, the spatial profiles of the beams become bigger, and the variation between positive and negative beams becomes more pronounced.

To investigate the possible systematic effect of laser beam spatial variations on electron polarization, the diffraction grating was removed, and the photocathode was illuminated with two linearly polarized Hermite-Gaussian laser beams, predominantly in the transverse electromagnetic (TEM) 00 mode, delivered one at a time, in a manner similar to that employed with the OAM beams. Using the "best practice" alignment procedure described above, an electron "polarization" of $0.48 \pm 0.06\%$ was measured. This measured value of 0.48% is symptomatic of the systematic error associated with the SAM polarization measurement due to beam misalignment. One beam was then purposely displaced relative to the other by a distance comparable to the beam diameter, and the polarization was remeasured. Successive one-diameter beam displacements mapped a square grid of a

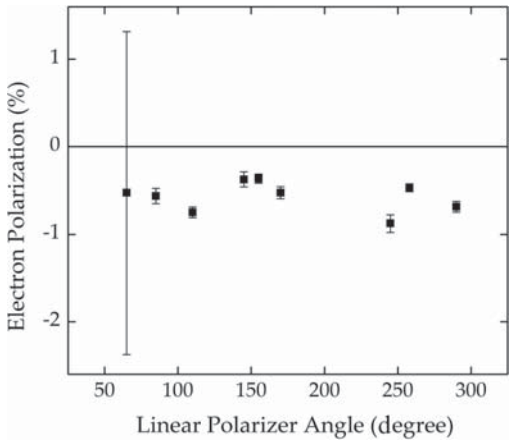

FIG. 9. Dependence of electron polarization on the angle of linear light polarization incident on the photocathode. The large error bar includes the composite (systematic and statistical) error of the asymmetry measurement as well as the error in S_{eff}. Subsequent error bars exclude systematic error (see text).

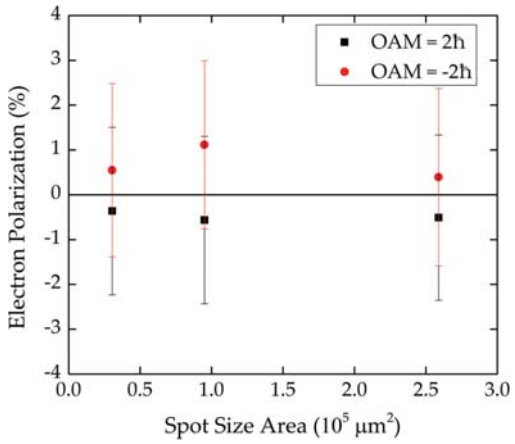

FIG. 10. (Color online) Dependence of electron polarization on laser spot size incident on the photocathode for $m = 2$. Statistical plus systematic errors (added linearly) are indicated.

size comparable to the intensity variations in the $m = 2$ OAM beams on the photocathode surface. The standard deviation of these polarization measurements was found to be 1.77% (absolute). This value is characteristic of the systematic error associated with the OAM polarization measurement caused by the spatial variation between positive and negative modes. Thus, laser beam misalignment was determined to be the dominant source of error.

V. CONCLUSIONS

The polarization of electrons emitted from bulk GaAs due to absorption of 789-nm light with OAM $= \pm 1\hbar, \pm 2\hbar, \pm 3\hbar$, and $\pm 5\hbar$ was measured and found to be consistent with zero with an upper limit of ~3%. This should be compared to a polarization using circularly polarized light of 32.32 ± 0.87(pol) ± 0.48(sys)%, where "pol" and "sys" refer to "polarization" (i.e., the uncertainty resulting solely from the Mott measurement) and "systematic" error, respectively. Specifically, taking the electron polarization P_e to be half the difference between that measured for the "+" and "−" OAM beams, we find that $P_e = 0.73 \pm 0.04(\text{pol}) \pm 1.77(\text{sys})\%$; $0.71 \pm 0.06(\text{pol}) \pm 1.77(\text{sys})\%$; $0.30 \pm 0.06(\text{pol}) \pm 1.77(\text{sys})\%$; and $0.16 \pm 0.06(\text{pol}) \pm 1.77(\text{sys})\%$ for $m = 1$, 2, 3, and 5 respectively.

The composite error for the OAM polarization measurements was found by adding the systematic error associated with beam misalignment to the error of the electron polarization measurements using beams with OAM. This latter error includes a linear sum of the statistical uncertainty of the polarization asymmetry measurement as well as the systematic uncertainty in S_{eff} ($\Delta E = 0$). The error bars presented in Figs. 8–10 for electron polarization include this final error. The composite error is completely dominated by the systematic error associated with spatial variations that occur in the centroid position and in the transverse intensity profile of the laser as the sign of the OAM is flipped. We assess an upper limit of 3.4% on electron polarization produced by OAM light incident on GaAs.

These null results, as well as the lack of obvious dependence of photocathode QE on m value, imply a relatively weak coupling between the OAM of the incident laser beam and the valance-band electrons of the GaAs bulk. As mentioned above, however, the hint of possible polarization for the $m = 1$ and 2 light might indicate some residual coupling. From the molecular theory,[11,13] we would expect the $m = 1$ coupling to be by far the strongest, given the exponential dependence on m of the transition probability P [Eq. (5)]. A definitive statement about such coupling strengths will obviously require more precise experiments. Further experiments investigating spin-polarized photoemission using OAM light from GaAs would consist principally of improvements to the optical system described in this report. Smaller beam sizes, on the order of several micrometers, are obtainable using high-numerical-aperture objective lenses.[10] Independently controlling OAM beams of opposite sign was principle in assessing the error of this experiment. Despite this, we note that the sign of the OAM may be reversed by other means. Insertion of a dove prism, for instance, would switch the sign of the OAM and alleviate some concern about dissimilar companion beams.[10]

Note added in proof. Recently, we communicated with G. F. Quinteiro concerning his theoretical studies of the absorption of OAM light by semiconductors. To calculate the probabilities for transitions involving OAM light he splits the transition matrix integral involving the inner product of the vector potential $\vec{A}$ and momentum operator $\vec{p}$ into a microscopic integral (within the unit cell of the semiconductor) and a macroscopic one (over the whole system). Because the vector potential is approximately constant within the unit cell, $\vec{A}$ appears only in the macroscopic integral. It is the microscopic integral that is used to calculate the valance-conduction band transitions probabilities. For this reason it is not expected in Quintero's theoretical formalism that OAM will have any influence on the photoemission yield.[23]

ACKNOWLEDGMENTS

We thank M. Fabrikant and A. Afanasev for independently proposing the experiment and C.J.G.J. Uiterwaal for useful discussions. P. Adderley, J. Clark, and M. Stutzman provided valuable assistance with the vacuum apparatus. This work was funded by the National Science Foundation through Grant No. PHY-0821385 and under US Department of Energy Contracts No. DE-AC05-84ER40150 and No. DE-FG02-97ER41025.

[1]L. Allen, M. W. Beijersbergen, R. J. C. Spreeuw, and J. P. Woerdman, Phys. Rev. A **45**, 8185 (1992).

[2]D. T. Pierce and F. Meier, Phys. Rev. B **13**, 5484 (1976).

[3]F. Meier, *Polarized Electrons in Surface Physics*, edited by R. Feder (World Scientific, Singapore, 1985), Chap. 10, pp. 423–466.

[4]Y. Poltoratska, R. Barday, U. Bonnes, M. Brunken, C. Eckardt, R. Eichhorn, J. Enders, C. Heßler, C. Ingenhaag, W. F. O. Müller, M. Platz, M. Roth, B. Steiner, M. Wagner, and T. Weiland, in *Proceedings of the 18th International Spin Physics Symposium*, AIP Conf. Proc. 1149, edited by D. G. Crabb, Y. Prok, M. Poelker,

S. Liuti, D. B. Day, and X. Zheng (AIP, New York, 2009), p. 983, and references therein.

[5]F. Zhou, A. Brachmann, T. Maruyama, and J. C. Sheppard, in *Proceedings of the 18th International Spin Physics Symposium*, AIP Conf. Proc. No. 1149, edited by D. G. Crabb, Y. Prok, M. Poelker, S. Liuti, D. B. Day, and X. Zheng (AIP, New York, 2009), p. 992, and references therein.

[6]M. Poelker, in *Proceedings of the Workshop on Polarized Electron Sources and Polarimeters*, AIP Conf. Proc. No. 1149, edited by D. G. Crabb, Y. Prok, M. Poelker, S. Liuti, D. B. Day, and X. Zheng (AIP, New York, 2009), p. 174, and references therein.

[7]K. Aulenbacher, Eur. Phys. J. Spec. Top. **198**, 361 (2012).

[8]H. He, M. E. J. Friese, N. R. Heckenberg, and H. Rubinsztein-Dunlop, Phys. Rev. Lett. **75**, 826 (1995).

[9]A. M. Yao and M. J. Padgett, Adv. Opt. Photonics **3**, 161 (2011).

[10]T. O'Neil, I. MacVicar, L. Allen, and M. J. Padgett, Phys. Rev. Lett. **88**, 053601 (2002).

[11]A. Alexandrescu, D. Cojoc, and E. DiFabrizio, Phys. Rev. Lett. **96**, 243001 (2006).

[12]S. J. van Enk, Quantum Opt. **6**, 445 (1994).

[13]M. Babiker, C. R. Bennett, D. L. Andrews, and L. C. Dávila Romero, Phys. Rev. Lett. **89**, 143601 (2002).

[14]M. Olszakier, E. Ehrenfreund, and E. Cohen, Phys. Rev. B **43**, 9350 (1991).

[15]G. F. Quinteiro and P. I. Tamborenea, Europhys. Lett. **85**, 47001 (2009).

[16]A. V. Carpentier, H. Michinel, J. R. Salgueiro, and D. Olivieri, Am. J. Phys. **76**, 916 (2008).

[17]V. Yu. Bazhenov, M. V. Vasnetsov, and M. S. Soskin, Pis'ma Zh. Eksp. Teor. Fiz. **52**, 431 (1990) [JETP Lett. **52**, 429 (1990)].

[18]V. Yu, Bazhenov, M. S. Soskin, and M. V. Vasnetsov, J. Mod. Opt. **39**, 985 (1992).

[19]N. R. Heckenberg, R. McDuff, C. P. Smith, H. Rubinsztein-Dunlop, and M. J. Wegener, Opt. Quantum Electron. **24**, S951 (1992).

[20]J. L. McCarter, M. L. Stutzman, K. W. Trantham, T. G. Anderson, A. M. Cook, and T. J. Gay, Nucl. Instrum. Methods Phys. Res., Sect. A **618**, 30 (2010).

[21]H. M. Al-Khateeb, B. G. Birdsey, T. C. Bowen, A. S. Green, M. E. Johnston, and T. J. Gay, Rev. Sci. Instrum. **70**, 3882 (1999).

[22]T. J. Gay and F. B. Dunning, Rev. Sci. Instrum. **63**, 1635 (1992).

[23]G. F. Quinteiro and P. I. Tamborenea, Phys. Rev. B **79**, 155450 (2009); private communication.